Chinese Chemical Letters 34 (2023) 107773

Contents lists available at ScienceDirect

Chinese Chemical Letters

journal homepage: www.elsevier.com/locate/cclet

A series of high-nuclear planar equilateral triangle-shaped $\{Ln_6(\mu_3\text{-}OH)_6\}$ cluster encapsulated polyoxoniobates with frequency dependent magnetic property

Zeng-Kui Zhu, Ya-Yun Lin, Rong-Da Lai, Xin-Xiong Li, Yan-Qiong Sun*, Shou-Tian Zheng*

State Key Laboratory of Photocatalysis on Energy and Environment, College of Chemistry, Fuzhou University, Fuzhou 350108, China

ARTICLE INFO

Article history:
Received 21 June 2022
Revised 15 July 2022
Accepted 22 August 2022
Available online 28 August 2022

Keywords:
Heteropolyoxoniobate
Hexanuclear iso-Ln-oxo cluster
Copper complexes
Water vapor adsorption
Ferromagnetism

ABSTRACT

The integration of lanthanide (Ln) ions and polyoxoniobates (PONbs) is challenging, and the known Ln-substituted PONbs are still scarce. This work introduces high-nuclear iso-Ln-oxo clusters into the PONb system. The first series of high-nuclear Ln-oxo clusters encapsulated heterometallic polyoxoniobates $H_9[Na(H_2O)_4][Cu(en)_2]_{10}\{Ln_6(\mu_3\text{-}OH)_6(SiNb_{18}O_{54})_3\}\cdot 18H_2O$ (**1-Ln**, en = ethylenediamine, Ln = Dy, Gd, Tb, Ho, Er, Tm, Yb, Lu) based on flower-like $\{Ln_6(\mu_3\text{-}OH)_6(SiNb_{18}O_{54})_3\}$ ($\{Ln_6Si_3Nb_{54}\}$) clusters have been successfully synthesized *via* one-pot hydrothermal synthesis strategy. The flower-like polyoxoanion $\{Ln_6Si_3Nb_{54}\}$ is consisted of three heteropolyoxoniobate $\{SiNb_{18}O_{54}\}$ clusters and one unique planar equilateral triangle-shaped $\{Ln_6(\mu_3\text{-}OH)_6\}$ cluster, which presents the highest nuclear iso-Ln-oxo cluster in PONb chemistry. In $\{Ln_6(\mu_3\text{-}OH)_6\}$ cluster, each pair of μ_3-OH groups link three Dy^{3+} ions to form a small approximate equilateral triangle-shaped $\{Dy_3(OH)_2\}$ cluster. Furthermore, the three $\{Dy_3(OH)_2\}$ clusters comprise a bigger approximate equilateral triangle-shaped $\{Dy_6(\mu_3\text{-}OH)_6\}$ cluster. The reported hexanuclear $\{Ln_6\}$ cluster skeletons are mostly octahedral, however, such equilateral triangle-shaped skeleton of the hexanuclear Ln-oxo cluster is first observed. The **1-Dy** exhibits good water vapor adsorption capacity and ferromagnetic properties.

The introduction of lanthanide (Ln) ions into polyoxometalates (POMs) to generate Ln-substituted POMs has attracted great interest, mainly due to their fascinating structural diversities and intriguing electronic, magnetic, and catalytic properties [1–6]. So far, a wealth of Ln-substituted POMs compounds with various compositions, shapes and sizes have been reported. However, the cases of high-nuclear Ln-substituted POMs were mainly obtained in polyoxotungstates (POTs) system, such as $\{[Ce_{10}O_6(OH)_6(CO_3)(H_2O)_{11}][(P_2W_{16}O_{59})]_3\}$ [7], $\{As_{12}Ce_{16}(H_2O)_{36}W_{148}O_{524}\}$ [8], $\{Ce_{20}Ge_{10}W_{100}O_{376}(OH)_4(H_2O)_{30}\}$ [9], $\{K_8Ce_{24}Ge_{12}W_{120}O_{444}(OH)_{12}(H_2O)_{64}\}$ [10], $\{Dy_{30}Co_8Ge_{12}W_{108}O_{408}(OH)_{42}(H_2O)_{30}\}$ [11], $\{Ln_{27}Ge_{10}W_{106}O_{406}(OH)_4(H_2O)_{24}\}$ (Ln = La and Ce) [12], and $\{Ln_{30}Ge_{12}W_{107}O_{420}(OH)_2(H_2O)_{14}\}$ (Ln = Sm and Eu) [13]. Compared with Ln-substituted POTs, the development of Ln-substituted polyoxoniobates (PONbs) is still in its infancy, which may be due to the narrow working pH range (10–12.5) and the low solubility of niobate species [14–19]. Up to now, only seven types of non-isomorphic Ln-substituted PONbs have been reported, including $\{Er\text{-}Nb_9CO_3\}$ [20], $\{Nd\text{-}Nb_{48}CO_3\}$ [20], $\{Ln_6M_2Nb_{30}\}$ (Ln = Eu, Er/Yb, Dy; M = Al, Cr, Mn, Fe, Co) [21–23], $\{Ln_{12}W_{12}Nb_{72}\}$ (Ln = Y, La, Sm, Eu, Yb) [24], $\{Ln_3Nb_{48}\}$ (Ln = Eu) [25], and two high-dimensional structures based on $\{Ln_3Nb_{48}\}$ (Ln = Dy and Eu) [26]. Among these compounds, only six Ln^{3+} ions in the $\{Ln_6M_2Nb_{30}\}$ can be joined together by oxygen atoms to form a triangular antiprismatic hexanuclear $\{Ln_6\}$ cluster, and further this $\{Ln_6\}$ cluster can be connected with two metal ions to form a 3p/3d-4f heterometallic cluster. However, apart from $\{Ln_6M_2Nb_{30}\}$, the Ln ions incorporated in these PONbs are spatially separated and magnetically isolated from each other by PONb polyoxoanions.

As is known to all, the integration of Ln ions and PONbs is challenging, and the known Ln-substituted PONbs are still scarce because of the suitable reaction conditions for PONb clusters are carried out under strong alkalinity (usually pH value > 10), under which Ln ions are more likely to precipitate as hydroxides. Considering the promising applications of Ln-substituted PONbs in the domains of luminescence, photocatalysis, base-catalyzed reactions, nuclear-waste treatment, magnetism, and *etc.* [14-19,27-30], introducing high-nuclear iso-Ln-oxo clusters into the PONb system is a very challenging and practical task. The majority of

* Corresponding authors.
E-mail addresses: sunyq@fzu.edu.cn (Y.-Q. Sun), stzheng@fzu.edu.cn (S.-T. Zheng).

https://doi.org/10.1016/j.cclet.2022.107773
1001-8417/

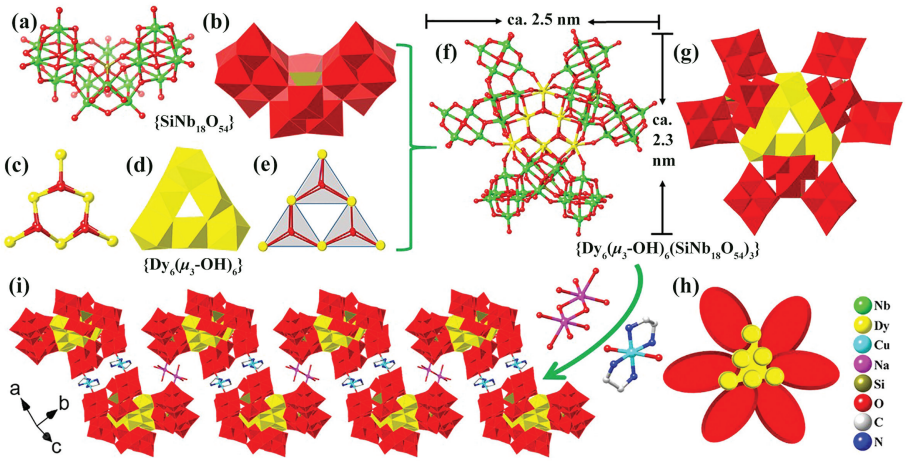

Fig. 1. (a, b) Polyhedral/ball-and-stick representations of $\{SiNb_{18}\}$ subunit. (c-e) Structures of $\{Dy_6(\mu_3\text{-}OH)_6O_{24}\}$ cluster. (f-h) View of the flower-like $\{Dy_6(\mu_3\text{-}OH)_6(SiNb_{18}O_{54})_3\}$ cluster. (i) View of the 1D wavy chain structure. Polyhedra key: SiO_4, olive; DyO_8, yellow; NbO_6, red.

hexanuclear $\{Ln_6\}$ cluster skeletons in hexalanthanide complexes are octahedral, while the *quasi*-planar hexagonal hexanuclear Ln_6 cluster was also observed in metal-organic frameworks materials [31]. Meanwhile, the trigonal antiprismatic hexanuclear Ln_6 clusters were observed in the reported Ln-containing POMs [32]. However, the equilateral triangle-shaped hexanuclear $\{Ln_6\}$ clusters have not been reported so far.

Herein, we report a series of unprecedented high-nuclear heterometallic PONb clusters $\{Ln_6(\mu_3\text{-}OH)_6(SiNb_{18}O_{54})_3\}$ ($\{Ln_6Si_3Nb_{54}\}$) (Ln = Dy, Gd, Tb, Ho, Er, Tm, Yb, Lu), with the following remarkable features: (1) The incorporated six Ln^{3+} ions in $\{Ln_6Si_3Nb_{54}\}$ form a rare hexanuclear planar equilateral triangle-shaped $\{Ln_6(\mu_3\text{-}OH)_6\}$ cluster, which is the largest number of iso-Ln-oxo cluster incorporated in PONb chemistry by far; (2) The PONb building cluster units in $\{Ln_6Si_3Nb_{54}\}$ are three identical siliconiobates $\{SiNb_{18}O_{54}\}$, which is first observed in Ln-containing PONbs; (3) The $\{Ln_6Si_3Nb_{54}\}$ clusters can be connected by $[Cu(en)_2]^{2+}$ complexes and Na_2O_2 clusters alternately, to form a 1D wavy chain running along the [011] direction, which is isolated as $H_9[Na(H_2O)_4][Cu(en)_2]_{10}\{Ln_6(\mu_3\text{-}OH)_6(SiNb_{18}O_{54})_3\}\cdot 18H_2O$ (**1-Ln**, en = ethylenediamine, Ln = Dy, Gd, Tb, Ho, Er, Tm, Yb, Lu).

Single-crystal X-ray diffraction analyses revealed that **1-Ln** are isostructural (Tables S1 and S2 in Supporting information), therefore, **1-Dy** is used as a representative example for depicting the crystal structure in detail. Compound **1-Dy** crystallizes in the triclinic space group *P*-1 and its asymmetric unit consists of two distinctive parts: three hetero-PONb clusters $\{SiNb_{18}O_{54}\}$ ($\{SiNb_{18}\}$) (Figs. 1a and b) and one planar equilateral triangle-shaped dysprosium-oxygen cluster $\{Dy_6(\mu_3\text{-}OH)_6O_{24}\}$ ($\{Dy_6\}$) (Figs. 1c-e). $\{SiNb_{18}\}$, as one of the classic $\{XNb_{18}O_{54}\}$ (X = Si, Ge, Al, Ga) hetero-PONb clusters [33–39], was first reported by Nyman group in 2011 [33]. The crescent-like $\{SiNb_{18}\}$ consists of two classical Lindqvist-type $\{Nb_6O_{19}\}$ units bridged by a unique B-type hexavacant $\{B\text{-}SiNb_6O_{26}\}$ Keggin fragment (Figs. 1a and b). In $\{SiNb_{18}\}$, the Si-O, Nb-O_t (t = terminal), Nb-O_b (b = bridging) and Nb-O_c (c = central) bond lengths are in the range of 1.617(9)–1.668(9) Å, 1.721(6)–1.773(0) Å, 1.7674–2.5262 Å and 2.177(6)–2.588(9) Å, respectively. These values are consistent with the reported values of $\{SiNb_{18}O_{54}\}$-based compounds [33–39]. In the most of the reported $\{XNb_{18}O_{54}\}$-based compounds, the $\{XNb_{18}O_{54}\}$ moities are directly connected by alkali metals ions or metal complexes to form extended structures, but it is not reported that the $\{XNb_{18}O_{54}\}$ moities can be used as secondary building units to aggregate high-nuclear metal-oxo clusters to generate novel heterometallic PONb clusters.

An interesting structural feature of **1-Dy** is the formation of hexanuclear planar equilateral triangle-shaped $\{Dy_6(\mu_3\text{-}OH)_6\}$ cluster. The six Dy^{3+} ions are almost coplanar and connected by six μ_3-OH groups. Each pair of μ_3-OH groups link three Dy^{3+} ions to form a small approximate equilateral triangle-shaped $\{Dy_3(OH)_2\}$ cluster (Figs. 1c-e). The three $\{Dy_3(OH)_2\}$ clusters comprise a bigger approximate equilateral triangle-shaped $\{Dy_6(\mu_3\text{-}OH)_6\}$ cluster, in which the three Dy^{3+} cations Dy4, Dy5, and Dy6 are arranged in the vertexes of the bigger equilateral triangle with the Dy-Dy distances of 7.07, 7.01 and 7.00 Å and the angle of ∠ Dy-Dy-Dy of 59.61°, 60.67° and 59.72°, respectively (Fig. S1 in Supporting information). These data show that the bigger triangle is an approximate equilateral triangle. The remaining three Dy^{3+} cations Dy1, Dy2, and Dy3 are located at the midpoint of each edge of the bigger approximate equilateral triangle (Fig. S1). To the best of our knowledge, such planar equilateral triangle-shaped $\{Dy_6(\mu_3\text{-}OH)_6\}$ has not been reported in POM chemistry. All the Dy^{3+} ions exhibit eight-coordinated distorted square antiprism geometry: some oxygen atoms from $\{SiNb_{18}\}$ clusters, the remaining oxygen atoms from μ_3-OH and the Dy-O bond distances range from 2.284(4)–2.595(6) Å (Fig. S2 in Supporting information). Furthermore, after bond valence sum calculations, the valence states of these μ_3-O atoms are all −1 (Table S3 in Supporting information), and six μ_3-O atoms are ultimately determined as six μ_3-OH groups (Fig. S3 in Supporting information).

The $\{Dy_6(\mu_3\text{-}OH)_6\}$ cluster is captured by three hetero-PONb $\{SiNb_{18}\}$ building blocks, where every linear Dy_3 cluster in the edge of the $\{Dy_6(\mu_3\text{-}OH)_6\}$ equilateral triangle is inset in the vacancy of hexavacant $\{B\text{-}SiNb_6O_{26}\}$ Keggin fragment of the $\{SiNb_{18}\}$ units to generate a novel flower-like high-nuclear Ln-oxo cluster embedded heterometal PONb trimer $\{Dy_6Si_3Nb_{54}\}$, with the dimensions $2.3 \times 2.5 \times 1.0$ nm^3 (Figs. 1f-h). In $\{Dy_6Si_3Nb_{54}\}$ cluster, the hetero-PONb cluster $\{SiNb_{18}\}$ is used for the first time to capture the high-nuclear Ln-oxo cluster, so $\{Dy_6Si_3Nb_{54}\}$ is a new type of Ln-substituted PONb based on hetero-PONb cluster $\{SiNb_{18}\}$ which is different from the reported iso-PONb-cluster-based Ln-substituted PONb [20–26]. A pair of centrosymmetric $\{Dy_6Si_3Nb_{54}\}$ moities are simultaneously bridged by a pair of $[Cu(en)_2]^{2+}$ (Cu8, Fig. S4 in Supporting information) to form a dimer of $\{Dy_6Si_3Nb_{54}\}$. These dimers are joint by Na_2O_2 clusters to generate a 1D wavy chain running along the [011] direction (Fig. 1i). Based on bond valence sum calculations, the oxidation states of all Nb, Dy, Si and Cu atoms were confirmed as +5, +3, +4 and +2, respectively (Tables S4-S7 in Supporting information). To balance the charge, an additional 9 proton hydrogens need to be added. These protons cannot

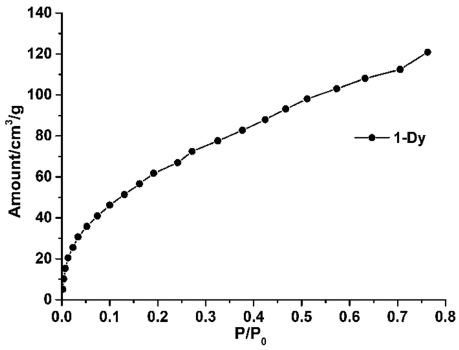

Fig. 2. Water vapor adsorption isotherm (298 K) of **1-Dy**.

be located and are assumed to be delocalized over the framework, which is a common phenomenon in POMs [40–42].

The phase purity of sample **1-Ln** can be confirmed by powder X-ray diffraction (PXRD) (Fig. S5 in Supporting information). Furthermore, the stability behavior of solid **1-Dy** in different pH and organic solvents was also tested. As shown in Fig. S6 (Supporting information), **1-Dy** can maintain its structural integrity with a wide pH range from 3 to 13. Further, **1-Dy** can also keep its structural stability in many organic solvents, such as DMF, DMA, CH_3CN, CH_3OH, C_2H_5OH, and isopropanol after soaking for 24 h (Fig. S7 in Supporting information). Thermogravimetric analysis (TGA) of **1-Ln** shows that the removal of guest molecules occurs in the temperature range of *ca.* 30–400 °C (Fig. S8 in Supporting information) and the PXRD patterns confirm that **1-Dy** maintains its crystallinity at least up to 200 °C (Fig. S9 in Supporting information). Solid-state diffuse reflectance UV–vis spectra of **1-Ln** show two strong absorption bands in the range of 200–380 nm and 420–800 nm, respectively (Fig. S10 in Supporting information). The absorption peak of 200–380 nm can be attributed to the charge transfer of O→Nb and the absorption peak of 420–800 nm can be ascribed to the d-d transition of incorporated 3d Cu^{2+} ions [17].

The calculation result with the PLATON program shows that the solvent-accessible volume per unit cell of **1-Dy** is 4413.8 Å^3 (31.0% of the total unit cell volume). Subsequently, N_2 and water sorption experiments were carried out to study its porosity. The N_2 adsorption isotherm at 77 K shows no absorption (Fig. S11 in Supporting information), while the water sorption isotherm at room temperature (298 K) proves that it has permanent microporosity. As shown in Fig. 2, the water absorption of **1-Dy** increased with increasing relative pressure, and all data provide the type I isotherm characteristic of a microporous solid. At $P/P_0 = 0.75$, **1-Dy** shows 120.87 cm^3/g (9.7 wt%) water vapor uptakes, which exhibits a relatively moderate water vapor adsorption capacity compared with other POMs (Table S8 in Supporting information).

1-Dy may show fascinating magnetic properties due to the single-ion orbital degeneracy of dysprosium atoms and the existence of equilateral triangle-shaped hexanuclear $\{Dy_6(\mu_3\text{-}OH)_6\}$ clusters in **1-Dy**. Under an external magnetic field of 1 kOe, the magnetic susceptibility of **1-Dy** was measured in the temperature range of 2–300 K. As shown in Fig. 3a, the experimental ($\chi_m T$) value at 300 K is 85.95 cm^3 K/mol, which is smaller than the theoretical value of 88.72 cm^3 K/mol for six Dy^{III} ions ($S = 5/2$, $g = 4/3$, $C = 14.17$ cm^3 K/mol) and ten Cu^{II} ions ($S = 1/2$, $g = 2$, $C = 0.37$ cm^3 K/mol). During the cooling process, the $\chi_m T$ value first decreases slightly and then begins to increase smoothly to the maximum value of 90.04 cm^3 K/mol at 16 K, which indicates the existence of ferromagnetic interactions [43,44]. With further cooling, the $\chi_m T$ value decreases sharply to a minimum of 83.40 cm^3 K/mol at 2 K, which indicates the existence of antiferromagnetic interactions in the range of 2–16 K (Fig. 3a) [45,46]. Furthermore, the tempera-

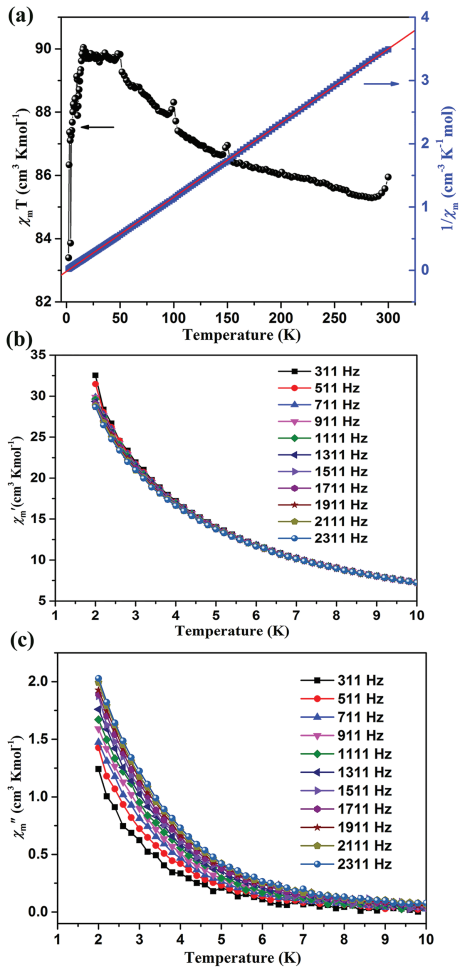

Fig. 3. (a) The temperature dependences of ($\chi_m T$) measured for **1-Dy**; (b, c) Frequency-dependent behavior of χ_m' and χ_m'' for **1-Dy** in zero static fields at 2–10 K, respectively.

ture (T) dependence of the reciprocal susceptibility ($1/\chi_m$) can be fitted with Curie-Weiss law at the temperature range of 2–300 K, with the Curie constants $C = 85.32$ cm^3 K/mol and $\theta = 1.535$ K for **1-Dy**, which further proves the existence of ferromagnetic interactions for **1-Dy** [43,44]. As far as we know, **1-Dy** is the third PONb compound with ferromagnetic properties [43,44].

Field-dependent isothermal magnetization $M(H)$ of **1-Dy** at 2 K displays a magnetization increase from 0 to 80 kOe. As shown in Fig. S13 (Supporting information), the M value rapidly increases to 40 $N\beta$ from 0 to 13 KOe at a very low field, and then gradually increases to the maximum value of 52.83 $N\beta$ at 80 kOe. The maximum value is less than the theoretical value of 70 $N\beta$ for six Dy^{III} and ten Cu^{II} (10 $N\beta$ for each Dy^{III} and 1 $N\beta$ for each Cu^{II}), which may be due to the crystal field effect on Dy^{3+} ions eliminating the degeneracy of the ground state [47,48].

The difference between the observed and expected magnetization saturation values indicates the existence of low excited states and/or magnetic anisotropy [49,50]. In order to explore whether the magnetic interaction in **1-Dy** can cause the behavior of single-molecule magnets (SMM), alternating-current (ac) magnetic susceptibility of **1-Dy** at frequencies between 311 Hz and 2311 Hz was performed under an external magnetic field of 3 Oe. As the frequency increases, the dependent in-phase (χ_m') signal shows a slight decline, but the out-of-phase (χ_m'') signal shows an obvious drop (Figs. 3b and c). The obvious frequency dependence effects of **1-Dy** suggest that **1-Dy** has slow magnetization relaxation,

which may be the characteristic of single-molecule magnet (SMM) behavior.

In summary, a series of unprecedented high-nuclear Ln-oxo clusters encapsulated heterometallic PONb clusters $\{Ln_6Si_3Nb_{54}\}$ (Ln = Dy, Gd, Tb, Ho, Er, Tm, Yb, Lu) have been constructed from one unique planar equilateral triangle-shaped hexanuclear $\{Ln_6(\mu_3\text{-}OH)_6O_{24}\}$ cluster and three hetero-PONb $\{SiNb_{18}O_{54}\}$ clusters. The $\{Ln_6Si_3Nb_{54}\}$ clusters contain the highest nuclear iso-Ln-oxo cluster in PONb chemistry, and the hetero-PONb cluster $\{SiNb_{18}O_{54}\}$ is used for the first time to stabilize the $\{Ln_6(\mu_3\text{-}OH)_6O_{24}\}$ clusters. The compound **1-Dy** also exhibits good water vapor adsorption capacity and ferromagnetic properties. This work provides a promising strategy to construct new high-nuclear Ln-oxo cluster-incorporated PONbs. These results enrich the very limited members of the lanthanide-containing PONb family, which opens new perspectives for developing novel PONb composite materials.

Declaration of competing interest

The authors declare that they have no known competing financial interests or personal relationships that could have appeared to influence the work reported in this paper.

Acknowledgement

We gratefully acknowledge the financial support from the National Natural Science Foundation of China (NSFC, Nos. 21971040, 21971039 and 21773029).

Supplementary materials

Supplementary material associated with this article can be found, in the online version, at doi:10.1016/j.cclet.2022.107773.

References

[1] T. Yamase, Chem. Rev. 98 (1998) 307–325.
[2] C. Boskovic, Acc. Chem. Res. 50 (2017) 2205–2214.
[3] J.W. Zhao, Y.Z. Li, L.J. Chen, G.Y. Yang, Chem. Commun. 52 (2016) 4418–4445.
[4] J.M. Clemente-Juan, E. Coronado, A. Gaita-Ariño, Chem. Soc. Rev. 41 (2012) 7464–7478.
[5] X. Liu, L. Cui, J. Jiang, Chin. Chem. Lett. 33 (2022) 2630–2634.
[6] J.W. Zhao, J.P. Wang, J.Y. Niu, Chin. Chem. Lett. 16 (2005) 1655–1658.
[7] P. Ma, R. Wan, Y. Wang, et al., Inorg. Chem. 55 (2016) 918–924.
[8] R.C. Howell, F.G. Perez, S. Jain, et al., Angew. Chem. Int. Ed. 40 (2001) 4031–4034.
[9] B.S. Bassil, M.H. Dickman, I. Römer, B. v. d. Kammer, U. Kortz, Angew. Chem. Int. Ed. 46 (2007) 6192–6195.
[10] S. Reinoso, M. Giménez-Marqués, J.R. Galán-Mascarlós, P. Vitoria, J.M. Gutiérrez-Zorrilla, Angew. Chem. Int. Ed. 49 (2010) 8384–8388.
[11] M. Ibrahim, V. Mereacre, N. Leblanc, et al., Angew. Chem. Int. Ed. 54 (2015) 15574–15578.
[12] Z. Li, X.X. Li, T. Yang, Z.W. Cai, S.T. Zheng, Angew. Chem. Int. Ed. 56 (2017) 2664–2669.
[13] Z. Li, Z.H. Lv, H. Yu, et al., CCS Chem. 4 (2022) 2938–2945.
[14] M. Nyman, F. Bonhomme, T.M. Alam, et al., Science 297 (2002) 996–998.
[15] M. Nyman, Dalton Trans. 40 (2011) 8049–8058.
[16] H.Y. Zhao, Y.Z. Li, J.W. Zhao, L. Wang, G.Y. Yang, Coord. Chem. Rev. 143 (2021) 213966.
[17] L. Jin, Z.K. Zhu, Y.L. Wu, et al., Angew. Chem. Int. Ed. 56 (2017) 16288–16292.
[18] Y.L. Wu, X.X. Li, Y.J. Qi, et al., Angew. Chem. Int. Ed. 57 (2018) 8572–8576.
[19] Z.K. Zhu, J. Zhang, Y.C. Cong, et al., Angew. Chem. Int. Ed. 61 (2022) e202113381.
[20] M. Amiri, N.P. Martin, C.L. Feng, J.K. Lovio, M. Nyman, Angew. Chem. Int. Ed. 60 (2021) 12461–12466.
[21] T. Ozeki, T. Yamase, H. Naruke, Y. Sasaki, Inorg. Chem. 33 (1994) 409–410.
[22] H. Naruke, T. Yamase, J. Alloy. Compd. 391 (2005) 302–306.
[23] Y.D. Lin, R. Ge, C.B. Tian, et al., Chem. Commun. 57 (2021) 8624–8627.
[24] L. Jin, X.X. Li, Y.J. Qi, P.P. Niu, S.T. Zheng, Angew. Chem. Int. Ed. 55 (2016) 13793–13797.
[25] S. Chen, P. Ma, H. Luo, et al., Chem. Commun. 53 (2017) 3709–3712.
[26] J. Zhang, R.D. Lai, Y.L. Wu, et al., Chem. Asian J. 15 (2020) 1574–1579.
[27] W. Guo, H. Lv, K.P. Sullivan, et al., Angew. Chem. Int. Ed. 55 (2016) 7403–7407.
[28] Z.K. Zhu, Y.Y. Lin, X.X. Li, D. Zhao, S.T. Zheng, Inorg. Chem. Front. 8 (2021) 1297–1302.
[29] Z.K. Zhu, Y.Y. Lin, L.D. Lin, et al., Inorg. Chem. 59 (2020) 11925–11929.
[30] Z.K. Zhu, L.D. Lin, J. Zhang, et al., Inorg. Chem. Front. 7 (2020) 3919–3924.
[31] G. Skorupskii, M. Dinca, J. Am. Chem. Soc. 142 (2020) 6920–6924.
[32] X. Fang, T.M. Anderson, C. Benelli, C.L. Hill, Chem. Eur. J. 11 (2005) 712–718.
[33] Y. Hou, M. Nyman, M.A. Rodriguez, Angew. Chem. Int. Ed. 50 (2011) 12514–12517.
[34] Y. Hou, T.M. Alam, M.A. Rodriguez, M. Nyman, Chem. Commun. 48 (2012) 6004–6006.
[35] P. Huang, C. Qin, X.L. Wang, et al., Dalton Trans. 41 (2012) 6075–6077.
[36] B.X. Liu, Z.W. Cai, T. Yang, et al., Inorg. Chem. Commun. 78 (2017) 56–60.
[37] J. Dopta, D.C. Krause, C. Näther, W. Bensch, Cryst. Growth. Des. 18 (2018) 4130–4139.
[38] Y.Y. Lin, J. Zhang, Z.K. Zhu, et al., Inorg. Chem. Commun. 113 (2020) 107766.
[39] Z.H. Zhong, J.X. Jing, Y.Q. Sun, X.X. Li, S.T. Zheng, Inorg. Chem. Commun. 132 (2021) 108813.
[40] Z.K. Zhu, Y.Y. Lin, H. Yu, X.X. Li, S.T. Zheng, Angew. Chem. Int. Ed. 58 (2019) 16864–16868.
[41] A.R.D.L. Olica, V. Sans, H.N. Miras, et al., Angew. Chem. Int. Ed. 51 (2012) 12759–12762.
[42] X. Fang, P. Kögerler, Y. Furukawa, M. Speldrich, M. Luban, Angew. Chem. Int. Ed. 50 (2011) 5212–5216.
[43] L. Li, Y. Niu, K. Dong, et al., RSC Adv. 7 (2017) 28696–28701.
[44] Z. Liang, D. Zhang, H. Wang, et al., Dalton Trans. 45 (2016) 16173–16176.
[45] Y.J. Wang, S.Y. Wu, Y.Q. Sun, X.X. Li, S.T. Zheng, Chem. Commun. 55 (2019) 2857–2860.
[46] B.S. Bassil, M. Ibrahim, R. Al-Oweini, et al., Angew. Chem. Int. Ed. 50 (2011) 5961–5964.
[47] Q. Zhang, J. Hu, Q. Li, et al., Chin. Chem. Lett. 33 (2022) 1417–1421.
[48] S. Osa, T. Kido, N. Matsumoto, et al., J. Am. Chem. Soc. 126 (2004) 420–421.
[49] P. Bag, C.K. Rastogi, S. Biswas, et al., Dalton Trans. 44 (2015) 4328–4340.
[50] A.S.R. Chesman, D.R. Turner, B. Moubaraki, et al., Dalton Trans. 41 (2012) 10903–10909.